

# Deep-Neural-Network-based anomaly detector for DC/DC power converter failure detection

Miguel Fernandez Costales\*<sup>1</sup>, Pablo F. Miaja<sup>1</sup>, Manuel Arias Perez de Azpeitia<sup>1</sup>, J. Antonio Fernandez<sup>1</sup>

<sup>1</sup>Power supply systems group - Department of Electrical, Electronic, Communication and Systems Engineering, University of Oviedo

The Electrical Power Subsystem (EPS) of a spacecraft is paramount to its operation since it will guarantee that every piece of equipment is receiving its required power. Therefore, the reliability of the power subsystem is one of the cornerstones of the full spacecraft reliability. DC/DC converters are one of the main constituents of the power subsystems. A method able to estimate the degradation of a dc-dc converter would enhance the power system reliability. It would allow to detect dc-dc converters prone to failure and to take corrective actions to extend their remaining lifespan.

## 1 Introduction

### 1.1 Electrical Power Subsystem

The Electrical Power Subsystem (EPS) is tasked with managing the electrical power sources inside a spacecraft, most commonly Solar Arrays (SA) and batteries, offering to the loads a reliable voltage. Many architectures are possible, being those cited in [1] the most typical ones. Figure 1 shows the regulated bus architecture in which the electrical power coming from the SA is regulated to a given voltage by means of the Solar Array Regulator. When there is not enough solar energy to provide the bus demand the battery energy is extracted to keep the bus voltage by means of the Battery Discharge Regulator (BDR). Finally, when there is available solar power and the battery needs its energy is replenished by means of the Battery Charge Regulator. At the core of the SAR, BDR and BCR there are DC/DC switching mode power converters that perform efficiently the electrical power conversion. [2] provides good insight in these pieces of equipment. Most DC/DC converters work by turning on and off (i.e. switching) several power switches. In the space electrical power domain, these switches are mostly MOSFET transistors and diodes. The most common kind of operation is to turn on and off the

MOSFETs at a constant frequency (100 kHz typically) and to control the fraction of time that the switch is on. This allows to control the current flowing in the power converter circuit and, thus, regulate the voltage at its output. It can be said that it controls the amount of energy that it is extracted from the input source. The fraction of time that the switch is on is called Duty cycle  $D$  so a MOSFET will be on for  $D \cdot T_s$  and off for  $(1 - D) \cdot T_s$ , then it will be turned on again for  $D \cdot T_s$  and the process will continue. The quantity  $T_s$  is the switching period. The control system of the DC/DC converter will act over  $D$  to keep the output variable controlled. Generally speaking this variable will be the output voltage or an internal current (generally an inductor current). At the end,  $D$  establishes the balance between the input and output energies. The input energy (extracted from the source) is always bigger than the one provided to the output (load). The reason for this is found in the circuit parasitics, generating power losses. This also affects  $D$ , which needs to be modified from the theoretical value to account for that extra lost energy.

One of the most prone to failure elements in a DC/DC converter are precisely the switching MOSFETs [3, 4]. When the MOSFET is on it presents a small resistance, called  $R_{on}$ . When the MOSFET degrades, this resistance increases, mostly due to thermomechanical effects. So most of the health monitor-

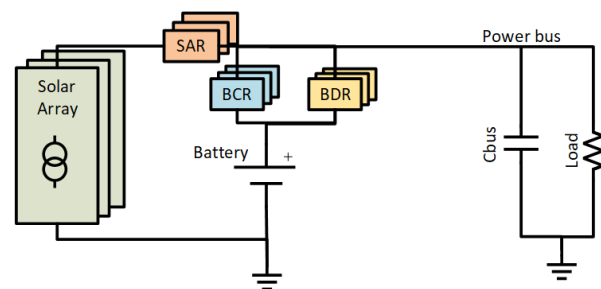


Figure 1: Satellite electrical power subsystem.

\*Corresponding author. E-Mail: fernandezcosmiguel@uniovi.es

ing techniques rely on estimating or measure this resistance [4]. Once this resistance increases, a certain amount (around 12% [5], however the same author claims a bigger value around 50% in [6]) from its initial value the MOSFET is considered prone to failure. However, this is not an easy task, since  $R_{on}$  depends on a lot of different variables, being the ambient temperature one of the most important. A high temperature makes the  $R_{on}$  to increase. Depending on the MOSFET, the increase in temperature could be bigger than the increase in  $R_{on}$  due to degradation. This  $R_{on}$  is one of the parasitics of the converter that will influence the duty cycle  $D$ . A methodology to estimate whether a converter is prone to failure would be of relevant importance in the Fault Detection, Isolation and Recovery (FDIR) concept.

## 1.2 Machine learning for Power Electronics

As almost every field of technology, power electronics has not escaped the advances in machine learning [7]. All the different domains within a power converter are quite complex and benefit from machine learning developments. Among them, optimization of power conversion systems [8, 9], magnetic elements modeling and design [10, 11] and of course health monitoring, including the effects of  $R_{on}$  like in [12, 13]. [14] uses the input and control variables of DC/AC converters to identify systems that are prone to failure.

In this paper an approach similar to [14] will be used. However, in this case it will be tried to determine whether a converter has degraded so it is close to failure or not. In digitally controlled DC/DC converters the determination of the control action (i.e duty cycle  $D$ ) is performed digitally from a series of digital conversions of samples of the relevant quantities, generally input and output voltages and internal currents (i.e. inductor currents). The goal would be to determine if a DC/DC converter is degraded from its control related measurements.

## 1.3 Anomaly detection

Anomaly detection is a class of system that can determine whether the system under observation is performing as intended or is functioning abnormally. There are many applications, even space-ones such as [15, 16]. One of the most used tools for this task is the autoencoder. The autoencoder [17] is a kind of neural network trained so its output  $\hat{x}$  matches its input  $x$ . The cornerstone of autoencoders is that in the middle of the network there is a hidden layer with a much smaller width than its input. This layer is often called

the bottleneck. The output of this layer is said to generate a code  $h$  that is dependent of the input. Therefore, it can be said that has two parts, the encoder function  $h = f(x)$  and the decoding one  $\hat{x} = g(h)$ . The autoencoder is trained in such a way that  $\hat{x} = g(f(x))$ . As  $h$  is much narrower the autoencoder learns the relevant information contained in  $x$ . In the frame of anomaly detectors the autoencoders are trained only with data,  $x$ , representing a good behavior of the system to be modelled. The error between  $x$  and  $\hat{x}$  should be very small. When under a certain input  $x_1$  the error exceeds a certain threshold an anomaly is claimed to be detected.

In DC/DC converters the control action is summarized in the duty cycle  $D$ . This control action takes into account the input and output voltages, the output current and all the parasitics, such as  $R_{on}$ . In this paper, instead of an autoencoder, but inspired by its working as anomaly detector, a feed-forward neural network will be trained to predict the  $\widehat{D}$  from a series of inputs. Given the relationship between  $D$  and the rest of the main parameters of the circuit, it was deemed as enough to obtain an accurate prediction. The duty cycle  $D$  contains all the relevant information in the same way the bottleneck layers work in an autoencoder. The autoencoder approach, recovering the inputs whilst narrowing the network, was tried and discarded. The duty cycle,  $D$ , is mostly determined by the ratio between input and output voltages. In fact, without considering losses it is just set by this ratio [2]. Then, recovering the input and output voltage from  $D$  is an under-determined problem, since there are many combinations of input and output voltage that give the same  $D$ . For implementing the approach, the inputs and  $D$  will be gathered during a qualification campaign modeling the behavior of a non-degraded DC-DC converter under foreseen operation conditions. With these data a feed-forward neural network is trained to predict  $\widehat{D}$ . The error in calculating  $\widehat{D}$  with the training data will be characterized by its average and standard deviation. In operation the inputs will be passed through the neural network to calculate  $\widehat{D}$ . When the error between the estimated  $\widehat{D}$  for a given input and the real one,  $D$ , exceeds the training error average by more than one standard deviation an anomaly will be decided. This implies that the real converter has deviated from the modeled one significantly. This is the scheme represented in Figure 2.

The anomaly detector is preferred over a neural network classifier. For classifier the network should be trained with examples of healthy and degraded DC/DC converters. Generating examples of degraded DC/DC converters is difficult and dangerous. Whilst in this paper only simulations will be carried out in a

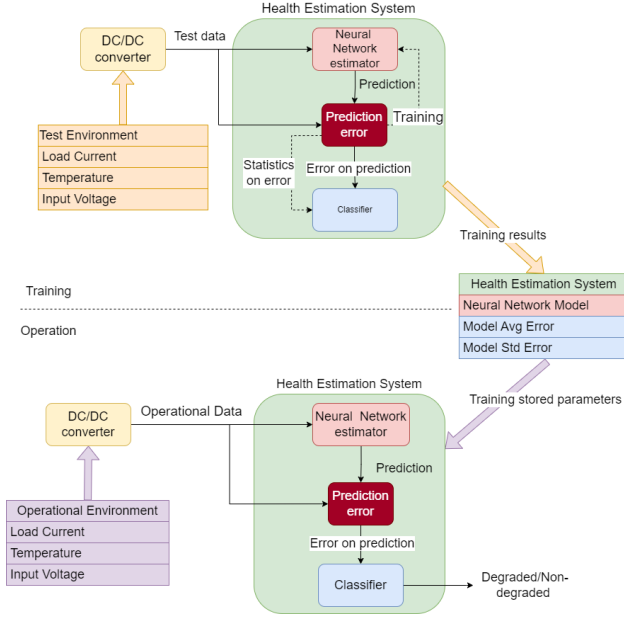


Figure 2: Anomaly detection scheme.

real application real DC/DC converter data must be used to train the networks. While it could be possible to artificially degrade the converters, that would be risky. Furthermore, it is possible that a new network shall be trained for every converter that will be monitored. In some way the neural network trained serves as a sort of digital-twin of the converter.

## 2 Generation of Data and Health monitoring system design

### 2.1 Data generation

The DC/DC converter used in [18] was simulated in the simulation software PSIM. The control described in [19] was also introduced in the simulation. These converters are controlled in an unconventional way. Instead of providing a fixed output voltage, they will provide a voltage dependent on the current supplied. It does so by forcing an internal current, the inductor current, to become a value  $I_{ref}$  set by a control loop. This  $I_{ref}$  is in turn controlled by adjusting  $D$ . This allows for an easier modularization of the system. From the neural network design point of view, it will be interesting since a new varying magnitude, the output voltage, is introduced. Then the output voltage  $V_{out}$  can serve as an input to the neural network.

The simulation model was enhanced introducing the  $R_{on}$  dependence on the MOSFET temperature as in [20]. In order to do so a reduced thermal model was used to simulate the internal temperature of each of the MOSFETs. This reduced model needs the theoret-

ical MOSFET losses as explained in [2] as well as a reference temperature  $T_{base}$ . A degradation model, introducing an increased  $R_{on}$  was also introduced. This degradation is just multiplying the nominal  $R_{on}$  by a factor  $1 + k_{deg}$ .

With this model two data-sets were generated. The first one models non-degraded converters over the full operation range. This is the data-set that will serve for training the neural network and characterizing the error statistics. Every point in this data-set will be labelled as "Non-degraded". The second data-set covers the same operation range but introduces increased  $R_{on}$  to model degraded converters. The DC/DC converter has 4 MOSFETs. The degradation is applied independently to each of them. When the simulation is performed with  $k_{deg} \geq 0.5$ , the data point will be labelled as degraded. This will mean an increase of 50% in the nominal  $R_{on}$  once affected by the temperature. The full training data-set is described by Table 1, as well as the data-set that includes degraded converters.

It is important to note that the simulation model may not be a faithful representation of the real converter. However, the simulation data will serve to determine if the proposed approach is enough to identify degraded converters and to determine what input variables will be the best ones to estimate  $\widehat{D}$ . The simulation model records the following parameters: Input voltage  $V_{in}(V)$ , Output voltage  $V_{out}(V)$ , Input current  $I_{in}(V)$ , Output current  $I_{out}(A)$ , Control current  $I_{ref}(A)$ , Duty cycle  $D$ , Temperature  $T_{base}(C)$ .

It is important to note that  $D$  is bounded between -1 and 1. The data will be recorded in floating point format. No considerations about the precision needed have been carried out at this stage of the work.

### 2.2 Neural Network Design

#### 2.2.1 Neural Network structure

The feed-forward neural network takes at its input the temperature  $T_{base}$ , input voltage,  $V_{in}$ , output voltage  $V_{out}$  and inductor current  $I_{ref}$ . The first layer of the network performs a normalization of the input

Param.	Non-Deg.	Step	Deg.	Step
$V_{in}$	[42, 100] V	1 V	[42, 100] V	5 V
$I_{out}$	[2, 6] A	0.25 A	[2, 6] A	1 A
$T_{base}$	[40, 70] °C	1 °C	[40, 70] °C	3 °C
$k_{deg}$	[0, 0.25]	0.25	[0, 0.9]	0.2

Table 1: Parameter ranges for non-degraded and degraded converters.

data. The network uses the *leakyRelu* activation function in all the hidden layers. Tensorflow [21] default parameters are used for this function. It has 13 layers. The maximum width is 29 neurons. Each 6 layers a normalization layer is introduced and the network is constrained to a width of 5. The total number of hidden layers is 13. The network has a single output and no activation function has been used for the output. No specific optimization of the neural network structure has been carried out. Figure 3 shows the implementation of this network.

Instead of training the network to predict  $D$  it will be trained to predict

$$D_{exp} = e^{1+D} \quad (1)$$

This allows maximizing the differences between predictions and eases the training and then the evaluation of the model.

### 2.2.2 Training the Neural Network

The neural network has been trained to fit  $D_{exp}$  defined in Equation (1). It will produce then  $\widehat{D_{exp}}$ . The chosen error function was the Mean Absolute Percentage Error (MAPE) this allows for maximizing the error in the cases in which  $D_{exp}$  is very small.

The typical split of the data of 80% for training and the remaining 20% for validation and testing is used. These data was selected from the simulation with non-degraded converters.

Finally, the network was trained using the Adam optimizer with a learning rate of  $1e-6$  and an epsilon of  $1e-7$ . To minimize the error, it was trained for more than 100000 epochs without showing over-fitting. The whole training data-set was used as batch size.

## 2.3 Classifier design

The health monitoring system of Figure 2 needs a classifier to determine whether the input data belongs to an anomaly or not. This decision is based in the Mean Absolute Error, defined as

$$MAE = \frac{1}{n} \cdot \sum_{i=1}^n D_{exp} - \widehat{D_{exp}} \quad (2)$$

Using the whole training data-set the output of the neural network is calculated and the MAE calculated. The average,  $\mu_{MAE}$  and standard deviation,  $\sigma_{MAE}$  of the MAE is calculated. The threshold is set to

$$th_{MAE} = \mu_{MAE} + \sigma_{MAE}, \quad (3)$$

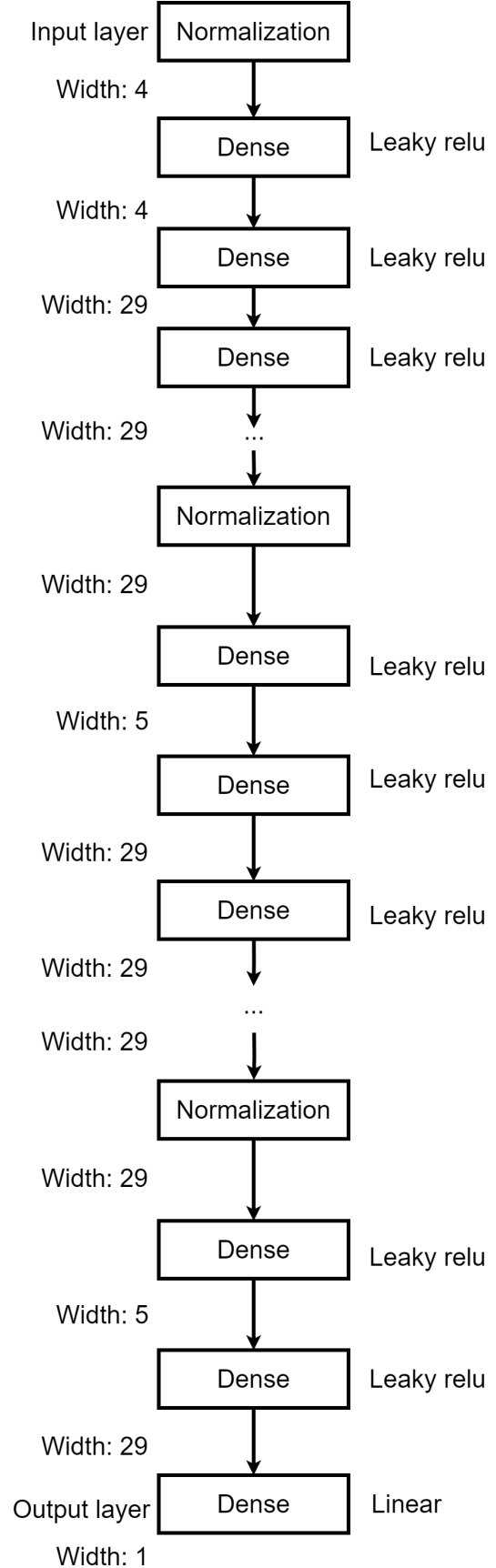


Figure 3: Implemented neural network.

### 3 Results

For estimating if a converter is degraded a sample of  $T_{base}$ ,  $V_{in}$ ,  $V_{out}$ ,  $I_{ref}$  and  $D$  is recorded. With  $D$  and Equation (1),  $D_{exp}$  is calculated. This forms a data point. Then, for this data point  $T_{base}$ ,  $V_{in}$ ,  $V_{out}$ ,  $I_{ref}$  are run through the neural network, obtaining  $\widehat{D}_{exp}$ . The error between  $\widehat{D}_{exp}$  and  $D_{exp}$  can then be calculated. In Figure 4, the MAE obtained after running the training dataset through the trained neural network is shown alongside the histogram of the MAE when running the test dataset, that includes the degraded converters. Given the distribution of values, a threshold  $th_{MAE}$  is defined, calculated as (Equation (3)). This threshold decides when a converter is degraded. Whenever  $th_{MAE} \leq |\widehat{D}_{exp} - D_{exp}|$  the sample will be labelled as belonging to a degraded converter. It can be seen how most of the training data lies below the threshold whilst a portion of the test data lies above the threshold.

The confusion matrix for the test dataset including the degraded converters is shown in Figure 5. The F-score is calculated to be 0.5677, due to having a considerable amount of False Positives with respect to True Positives. The scores show a balanced accuracy of 74.35%.

### 4 Discussion

The work presented in this paper shows an attempt to include a non-invasive anomaly detector for digitally controlled DC/DC converters. The results presented, using simulated data, show that the task is possible with moderate good results.

However, much more work is needed. The most relevant would be to use data from real DC-DC converters. This data will be used to train the neural network.

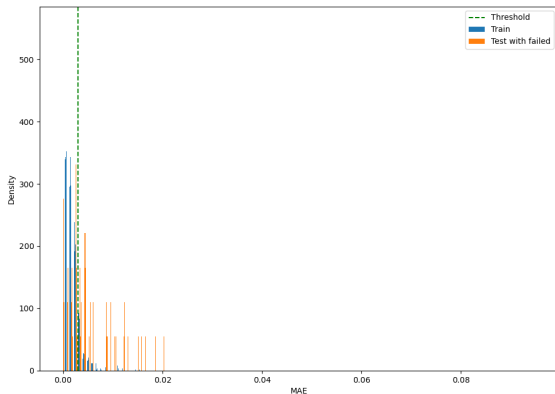


**Figure 4:** Histogram on the Mean Absolute Error between predicted  $\widehat{D}_{exp}$  and measured  $D_{exp}$ .

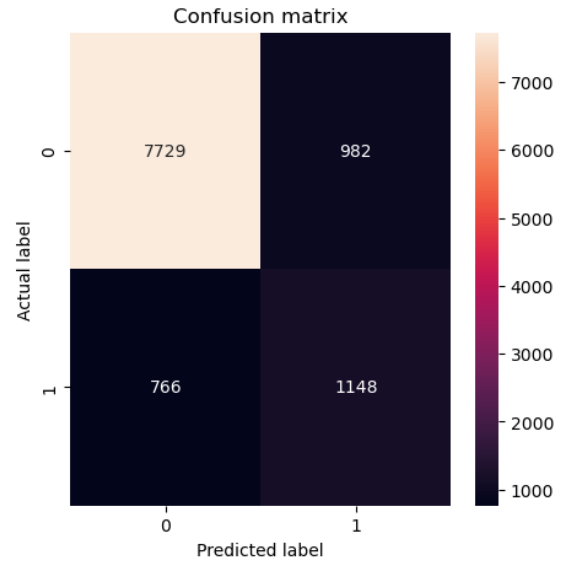


**Figure 5:** Confusion matrix between degraded and non-degraded converters based on the difference between NN predicted  $\widehat{D}$  and measured  $D$ .

Also, a deep study on the resolution needed for the task and its compatibility with the current control devices needs to be carried out. On top of that an optimization of the neural network and training process needs to be assessed.

The presented neural network is small by today's standards. However it needs to be studied if it could be fitted on-board. Whether inside the controlling elements for DC/DC converters or as part of the on-board software. Another possibility would be to implement it on ground, as part of an enhanced telemetry processing. In case of being processed by the on-board software the impact of such implementation on the on-board computer and in the data bus needs to be assessed. In case of implemented on ground the impact on the Telemetry and Telecommand Systems must be analyzed. In both cases strategies for deciding how often the samples for health estimation purposes must be taken need to be devised.

In summary, this work represents a first step in utilizing these techniques for electrical power subsystem monitoring.

### Acknowledgment

This work has been funded by the Spanish Ministry of Science through PID2021-127707OB-C21 and by the Principality of Asturias through PA-23-BP21-207.

## References

1. Patel, M. R. *Spacecraft Power Systems* ISBN: 978-0-8493-2786-5 (CRC Press, Boca Raton, 2005).
2. Erickson, R. W. & Maksimović, D. *Fundamentals of Power Electronics* Third edition. ISBN: 978-3-030-43879-1 (Springer, Cham, 2020).
3. Ferreira Costa, L. & Liserre, M. Failure Analysis of the Dc-Dc Converter: A Comprehensive Survey of Faults and Solutions for Improving Reliability. *IEEE Power Electronics Magazine* **5**, 42–51. ISSN: 2329-9207, 2329-9215. (2024) (Dec. 2018).
4. Hosseinabadi, F. *et al.* A Comprehensive Overview of Reliability Assessment Strategies and Testing of Power Electronics Converters. *IEEE Open Journal of Power Electronics* **5**, 473–512. ISSN: 2644-1314 (2024).
5. Dusmez, S. *et al.* Aging Precursor Identification and Lifetime Estimation for Thermally Aged Discrete Package Silicon Power Switches. *IEEE Transactions on Industry Applications* **53**, 251–260. ISSN: 1939-9367 (Jan. 2017).
6. Dusmez, S., Bhardwaj, M., Sun, L. & Akin, B. A Software Frequency Response Analysis Method to Monitor Degradation of Power MOSFETs in Basic Single-Switch Converters in 2016 *IEEE Applied Power Electronics Conference and Exposition (APEC)* (Mar. 2016), 505–510.
7. Zhao, S., Blaabjerg, F. & Wang, H. An Overview of Artificial Intelligence Applications for Power Electronics. *IEEE Transactions on Power Electronics* **36**, 4633–4658. ISSN: 1941-0107 (Apr. 2021).
8. Goodrick, K. J., Butler, A., Byrd, T. & Maksimović, D. *Machine Learning Estimators for Power Electronics Design and Optimization in 2021 IEEE Design Methodologies Conference (DMC)* (July 2021), 1–8.
9. Reese, S., Byrd, T., Haddon, J. & Maksimovic, D. *Machine Learning-based Component Figures of Merit and Models for DC-DC Converter Design in 2022 IEEE Design Methodologies Conference (DMC)* (Sept. 2022), 1–6.
10. Guillod, T., Papamanolis, P. & Kolar, J. W. Artificial Neural Network (ANN) Based Fast and Accurate Inductor Modeling and Design. *IEEE Open Journal of Power Electronics* **1**, 284–299. ISSN: 2644-1314 (2020).
11. Li, H., Serrano, D., Wang, S. & Chen, M. MagNet-AI: Neural Network as Datasheet for Magnetics Modeling and Material Recommendation. *IEEE Transactions on Power Electronics*, 1–17. ISSN: 1941-0107 (2023).
12. Mohagheghi, S., Harley, R. G., Habetler, T. G. & Divan, D. Condition Monitoring of Power Electronic Circuits Using Artificial Neural Networks. *IEEE Transactions on Power Electronics* **24**, 2363–2367. ISSN: 1941-0107 (Oct. 2009).
13. Zhao, S., Peng, Y., Zhang, Y. & Wang, H. Parameter Estimation of Power Electronic Converters With Physics-Informed Machine Learning. *IEEE Transactions on Power Electronics* **37**, 11567–11578. ISSN: 1941-0107 (Oct. 2022).
14. Yüce, F. & Hiller, M. Condition Monitoring of Power Electronic Systems Through Data Analysis of Measurement Signals and Control Output Variables. *IEEE Journal of Emerging and Selected Topics in Power Electronics* **10**, 5118–5131. ISSN: 2168-6785 (Oct. 2022).
15. *How Airbus Detects Anomalies in ISS Telemetry Data Using TFX* (2024).
16. *On-Board Anomaly Detection From The Ops-Sat Telemetry Using Deep Learning | Nebula Public Library* <https://nebula.esa.int/content/board-anomaly-detection-ops-sat-telemetry-using-deep-learning>. (2023).
17. Goodfellow, I., Bengio, Y. & Courville, A. *Deep Learning* <http://www.deeplearningbook.org> (MIT Press, 2016).
18. Fernandez, M. *et al.* Four-Switch Buck-Boost Based Module Block for Highly Modular Power Architecture in 2023 *13th European Space Power Conference (ESPC)* (2023), 1–6.
19. Zumel, P. *et al.* Digital Control for a Modular System of DC/DC Converters for Primary Distribution System in 2023 *13th European Space Power Conference (ESPC)* (2023), 1–6.
20. Dušan Graovac, M. P. & Andreas Kiep. *MOSFET Power Losses Calculation Using the DataSheet Parameters*
21. *API Documentation | TensorFlow v2.16.1* [https://www.tensorflow.org/api\\_docs](https://www.tensorflow.org/api_docs). (2024).